Structural Comparison of Two Major *endo*-1,4-Xylanases from *Trichoderma reesei*[†,‡]

Anneli Törrönen and Juha Rouvinen*

Department of Chemistry, University of Joensuu, P.O. Box 111, FIN-80101 Joensuu, Finland

Received August 24, 1994; Revised Manuscript Received November 10, 1994[⊗]

ABSTRACT: Three-dimensional structures of two major *endo*-1,4-xylanases, XYNI and XYNII from *Trichoderma reesei*, have been determined by X-ray crystallography. The amino acid sequences of both enzymes are highly homologous (identity approximately 50%), and both XYNI and XYNII exist as a single domain that contains two mostly antiparallel β-sheets which are packed against each other. The β-sheet structure is twisted, forming a cleft where the active site is situated. Two glutamic acids in the cleft, Glu75 and Glu164 in XYNI as well as Glu86 and Glu177 in XYNII, are most likely involved in catalysis. Inspection of the structures reveals that the width of the active site cleft and the number of subsites are different in XYNI and XYNII. The active site is narrower in XYNI and probably contains only three subsites, whereas the number of subsites in XYNII is most likely five. Variations in the surroundings of catalytic residue $Glu164_{XYNI}$/$Glu177_{XYNII}$ are thought to explain the pH optimum differences observed in XYNI and XYNII.

Many microorganisms are known to produce multiple forms of different 1,4-glycosidases in order to hydrolyze plant polysaccharides, i.e., mainly cellulose and xylan, which is the most abundant hemicellulose in nature. Xylan, composed of 1,4-linked xylanopyranoside units, is a more heterogeneous substrate than cellulose. It does not form microfibrils like cellulose, and its backbone may contain a number of substituents such as 4-*O*-methylglucuronic acid, L-arabinose, and *O*-acetyl groups. Because of the complex structure of the substrate, different glycosidases are needed to complete polysaccharide hydrolysis (Sundberg & Poutanen, 1991).

1,4-Glycosidases are classified as endo- and exoenzymes depending on their ability to catalyze the backbone breakage of their polymeric substrate. Exoenzymes prefer to hydrolyze the 1,4-glycosidic linkages from the ends of the polymeric chain, whereas endoenzymes prefer the internal bonds in the middle of the chain. Recent crystallographic studies have suggested that the active site in exoenzymes is situated in a tunnel, whereas in endoenzymes it is located in a cleft (Rouvinen et al., 1990; Divne et al., 1994).

A large number of amino acid sequences of different 1,4-glycosyl hydrolases are known. Hydrophobic cluster analysis first revealed eight families of 1,4-glycosidases (A−H) (Gilkes et al., 1991; Henrissat, 1991) and later eleven (A−K) (Henrissat & Bairoch, 1993). The total number of classified glycosyl hydrolase families (EC 3.2.1.*x*), is 45 (Henrissat et al., 1993).

In the last few years the number of solved three-dimensional structures of 1,4-glycosylases has increased rapidly. The structures of the catalytic domain of cellobiohydrolase II (family B/6) from *Trichoderma reesei* (Rouvinen et al., 1990), the catalytic domain of endoglucanase E2 (family B/6) from *Thermomonospora fusca* (Spezio et al., 1993); the catalytic domain of cellobiohydrolase I (family C/7) from *Trichoderma reesei* (Divne et al., 1994); endoglucanase CelD (family E/9) from *Clostridium thermocellum* (Juy et al., 1992); endoxylanases (family G/11) from *Bacillus pumilus* (Okada, 1989), *Bacillus circulans* (Campbell et al., 1993; Wakarchuk et al., 1994), and *Trichoderma harzianum* (Campbell et al., 1993); endoxylanase II (family G/11) from *Trichoderma reesei* (Törrönen et al., 1994); endoglucanase V (family K/45) from *Humicola insolens* (Davies et al., 1993); *Bacillus* H(A16-M) hybrid 1,3−1,4-glucanase (family 16) (Keitel et al., 1993); and two β-glucan endohydrolases from barley (Varghese et al., 1994) have been reported. These studies have revealed different folds and significant variations in the active site construction among enzymes from different families. However, the way in which smaller local differences in the three-dimensional structure contribute to the functional properties among structurally similar proteins within one family has been studied less.

We have recently determined the three-dimensional structure of *endo*-1,4-xylanase II (XYNII)[1] from *Trichoderma reesei*, which belongs to the highly specific and homologous xylanase family G/11 (EC 3.2.1.8). It is a one-domain molecule composed of 190 amino acid residues. It folds into two β-sheets which are packed against each other. The two β-sheets are strongly twisted and form a cleft on one side, which is an obvious suggestion of an active site. The structure also contains an α-helix. The fold is unique and thus far has only been observed in the G/11 family of xylanases. However, the structure shares some similarities with that of 1,3−1,4-glucanase from *Bacillus* (Keitel et al., 1993), which on the other hand resembles the structures of plant legume lectins and the recently solved structure of the core protein of cellobiohydrolase I from *Trichoderma reesei* (Divne et al., 1994). A striking feature was the observation

† Supported by the Academy of Finland.

‡ Crystallographic coordinates have been deposited in the Brookhaven Protein Data Bank (reference 1XYO, 1XYN, 1ENX, 1XYP).

* To whom correspondence should be addressed.

⊗ Abstract published in *Advance ACS Abstracts,* December 15, 1994.

[1] Abbreviations: XYNI, *endo*-1,4-xylanase I; XYNII, *endo*-1,4-xylanase II; PEG, poly(ethylene glycol); HCA, hydrophobic cluster analysis.

0006-2960/95/0434-847$09.00/0

Table 1: Crystal and Diffraction Data

	protein				
	XYNI	XYNI	XYNII	XYNII	XYNII
pH	4.2	4.5	4.5	6.0	6.5
precipitant	$(NH_4)_2SO_4$	PEG6000	$(NH_4)_2SO_4$	$(NH_4)_2SO_4$	$(NH_4)_2SO_4$
no. of crystals	1	1	1	1	1
space group	*C*2	*C*2	$P2_1$	$P2_1$	$P2_1$
a (Å)	71.9	72.25 (8)	81.55 (6)	81.55 (5)	81.82 (8)
b (Å)	39.0	39.01 (7)	60.64 (4)	60.80 (2)	60.90 (4)
c (Å)	59.9	54.30 (8)	38.25 (2)	38.15 (2)	38.13 (4)
β (deg)	118.0	91.80 (9)	94.46 (4)	94.38 (2)	94.43 (3)
max. resolution (Å)	2.5	2.0	1.5	1.5	1.5
reflns collected	7640	20 294	78 692	86 310	90 097
unique reflns	3703	7631	41 141	46 045	39 973
completeness (%)	72	79	68	76	66
R_{merge} (%)[a]	7.39	8.97	7.78	9.16	8.55

[a] $R_{merge} = 100 \times \Sigma\Sigma|F^2(i) - \langle F^2(i)\rangle|/\Sigma\Sigma F^2(i)$.

Table 2: Summary of Refinement

	protein			
	XYNI	XYNII	XYNII	XYNII
pH	4.5	4.5	6.0	6.5
resolution of data (Å)	8.0−2.0	8.0−1.5	8.0−1.5	8.0−1.5
reflns used ($F_o > 1\sigma$)	7475	40 728	45 625	39 560
R-factor (%)	18.5	19.0	19.3	18.9
no. of non-H atoms	1429	3231	3276	3288
protein	1348	2 × 1480	2 × 1485	2 × 1480
water	80	271	306	328
calcium	1			
deviation from ideality				
bond lengths (Å)	0.007	0.008	0.009	0.008
bond angles (deg)	1.5	1.6	1.6	1.6
dihedrals (deg)	26.8	27.2	27.2	27.3
improper dihedrals (deg)	1.1	1.2	1.2	1.2
av *B*-factors (Å^2)	18.76	17.81	16.92	17.26
main-chain atoms	16.65	14.73	13.80	14.14
all protein atoms	17.76	16.26	15.15	15.39
water	35.78	34.70	34.10	33.14
PDB code	1XYN	1XYO	1ENX	1XYP

[a] *R*-factor = $(\Sigma|F_o - F_c|)/\Sigma F_o$.

that XYNII seems to have two different conformational stages at pH 5.0 and 6.5 (Törrönen et al., 1994).

We now report the X-ray structure of another family G xylanase, *endo*-1,4-xylanase I (XYNI) from the same organism. The amino acid homology between XYNI and XYNII is 50%. However, their molecular and functional properties clearly differ. XYNI is a smaller protein (178 amino acids) than XYNII (190 amino acids). The isoelectric point of XYNI is 5.2, and that of XYNII is 9.0. The pH optimum is between 3.0 and 4.0 for XYNI and between 5.0 and 5.5 for XYNII. Biely et al. (1993) have recently reported that XYNI and XYNII have tendencies to hydrolyze xylo-oligomers in different ways. In this work we compare the three-dimensional structures of XYNI and XYNII and study the structure/function relationships of these enzymes.

EXPERIMENTAL PROCEDURES

Crystallization and Data Collection. The crystallization of XYNI and XYNII using ammonium sulfate as precipitant proceeded as described earlier (Törrönen et al., 1993b). However, the XYNI crystals obtained from ammonium sulfate were in most cases badly twinned or very small, and it was possible to collect the data set only to 2.5-Å resolution. This data set contained only about 3700 unique reflections (Table 1), making the structure refinement very difficult. A new crystal form for XYNI was obtained from poly(ethylene glycol). These new XYNI crystals were obtained by the hanging drop method, where 10-μL droplets consisted of 5 μL of a protein solution (10 mg/mL in 50 mM sodium acetate buffer, pH 4.5) and a 5-μL reservoir (20% PEG 6000 and 50 mM sodium acetate buffer, pH 4.5). These XYNI crystals from PEG also had a strong tendency to grow as twins. However, we could manage to collect a data set at 2.0-Å resolution. The unit cell dimensions are given in Table 1. The space group was confirmed to be *C*2 by means of the XPREP program (Shelxtl program package).

All data sets were collected on an R-AXIS IIC area detector (Sato et al., 1992) mounted on a Rigaku RU200HB rotating anode (Cu Kα radiation, 50 kV, 180 mA) and processed using R-AXIS IIC software. The data collection statistics are given in Table 1.

Structure Determination and Refinement. Phasing by multiple isomorphous replacement, model building, and initial refinement and the observation of two different conformational stages (at pH 5.0 and 6.5) for XYNII have been described earlier (Törrönen et al., 1994). XYNII crystallizes in the space group $P2_1$ and has two molecules (A and B) in an asymmetric unit. To better characterize the conformational change, new data sets for XYNII were collected at pH 4.5, 6.0, and 6.5. Crystals of different pHs were obtained by soaking native XYNII crystals (grown at pH 4.5) overnight in a precipitant solution where the pH was adjusted. New data sets were collected, and the resulting structures were refined by using the program X-PLOR (Brünger et al., 1990), all to 1.5-Å resolution. The relative occupancies of two different conformations of Glu177 at pH 6.0 were evaluated by the same program. The results of the refinements of all three XYNII structures are given in Table 2. The maximum *B*-factor allowed for water molecules was 60 Å^2. Two residues, Thr170 and Tyr181, were outside the allowed regions in the Ramachandran plot (Ramakrishnan & Ramachandran, 1965) (Figure 1).

The structure of XYNI was solved by the molecular replacement method, which in this particular case proved to be quite straightforward. In the beginning, only XYNI crystals from ammonium sulfate were available for the structure determination. The XYNII model, into which XYNI amino acid sequence changes were incorporated by program O (Jones et al., 1991), was used as a search model. All the diffraction data with F > 2σ in the resolution range from 8.0 to 4.0 Å were used in the rotation and translation functions in X-PLOR (Brünger, 1990). The data from the first XYNI crystals gave a rotation function solution with a 9.0σ peak height and a translation function with a 13.6σ peak height. It was possible by using the resulting model to determine the position of the protein main chain and the conformations of many side chains. However, the small number of unique reflections did not allow the addition of water molecules. The temperature factors for all protein atoms were also fixed at the value of 18.0 Å^2. In total, eight cycles of modeling and subsequent refinement with the programs O and X-PLOR reduced the crystallographic *R*-factor to 21.2%. This XYNI model was later used as a search model for solving the structure from XYNI crystals obtained from poly(ethylene glycol). No rotation was observed between the protein molecules in the two XYNI

crystal forms (peak height, 10.1σ), and the translation function showed a clear peak at the height of 22.4σ (vector length, 33.7 Å).

The initial $2|F_o| - |F_c|$ electron density map calculated at 2.0-Å resolution for the XYNI structure (crystals from PEG) was good, and almost all secondary structure elements were well defined. Only some loop regions had an uninterpretable density. Visual inspection of intermediate models and manual rebuilding were carried out with program O (Jones et al., 1991), and all the structures were refined with the program X-PLOR (Brünger et al., 1987). Energy minimization using parameters derived from the Cambridge data base of small molecule structures (Engh & Huber, 1991) was used in refinement cycles. Individual temperature factors were refined at later steps. The initial model had an *R*-factor of 40%, and water molecules were added once the *R*-factor value was under 22%. The final model contains 80 water molecules and one calcium ion, which was found to bind to Asp81 and His83 on the surface of the protein. The maximum *B*-factor allowed for water molecules was 60 Å^2. The final refinement statistics for XYNI refinement are given in Table 2. Two residues, Ser2 and Gln157, were outside the allowed regions in the Ramachandran plot (Ramakrishnan & Ramachandran, 1965) (Figure 1).

Soaking Experiments. In order to better determine substrate binding, several attempts were made by soaking XYNII crystals in different ligand solutions at various pHs. These ligands included xylose, xylobiose, xylotriose, xylotetraose, xylopentaose, *p*-nitrophenylthioxylobioside and *p*-chlorophenyl thioxylobioside. No clear electron density was observed for any ligand. We attempted to conclude whether the tested ligands had too low an affinity for the enzyme or the hydrolysis of the ligand (longer xylooligomers) was catalyzed too rapidly. When examining the packing of XYNII molecules, we concluded that the active site is easily accessible to the solvent channels. The packing probably has no influence on the conformational change, which is also supported by the fact that unit cell dimensions between different measured XYNII structures were almost equal. On the other hand, in XYNI crystals the packing of molecules may hinder ligand binding. Several cocrystallization attempts for both XYNI and XYNII were performed, but only twinned crystals were obtained.

The only experiment which produced some observable electron density for ligands involved soaking the XYNII crystal in a pretreated oat spelts xylan (purchased from FLUKA) solution. This xylan is a heteropolysaccharide and contains glucuronic acid and acetic acid substituents. The xylan (1 mg/mL in 50 mM sodium acetate buffer, pH 5.3) was partly hydrolyzed with XYNII (100 milliunits/mL) for 2 min at 50 °C, and the reaction was stopped by placing the sample into boiling water for 5 min. This partial hydrolysis produced a solution which contained soluble and insoluble substituted xylo oligomers of different lengths. These xylo oligomers were supposed to have a much higher binding affinity than unsubstituted short oligomers. This solution was used without further purification when native XYNII crystals at pH 5.3 (corresponding to the pH optimum of XYNII) were soaked for 3 h. The data set was collected at 2.0-Å resolution, and the native XYNII model was used in the refinement. The $2|F_o| - |F_c|$ electron density map was calculated over a different range of low-resolution data, but the use of the resolution range 2.0−8.0 Å produced the clearest electron density for the ligand (crystallographic *R*-factor, 16.7%). Because of the heterogeneity of xylan, no ligand model was used in the refinement.

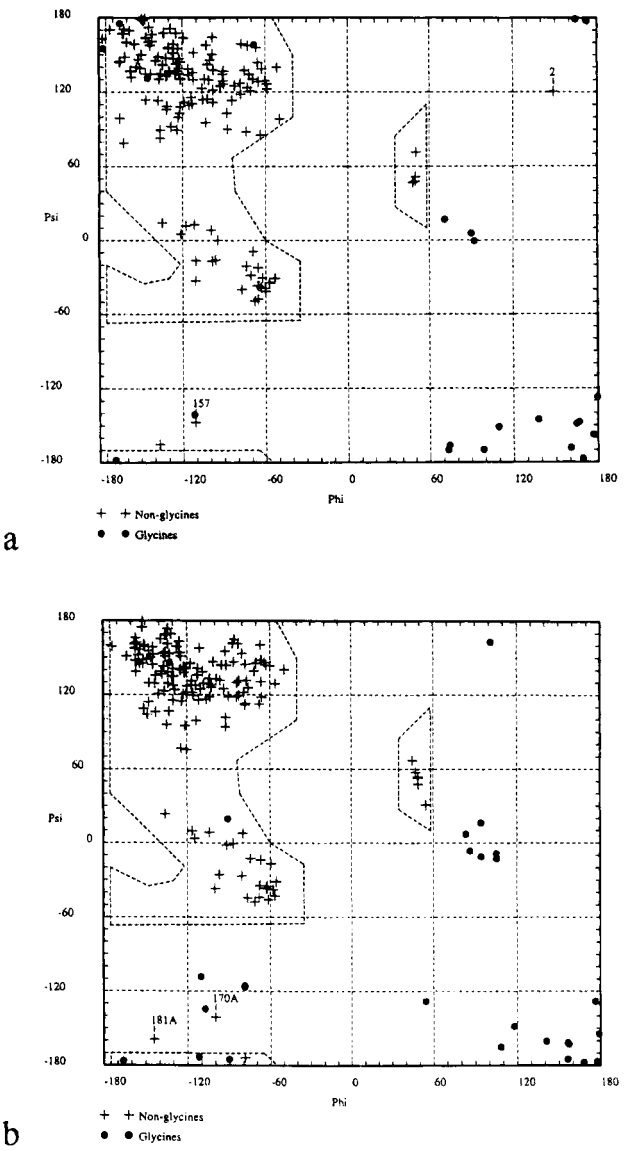

FIGURE 1: Ramachandran plots for the final models of (a) XYNI and (b) XYNII, molecule A.

RESULTS

Overall Structures of XYNI and XYNII. The overall structure of XYNI clearly resembles that of XYNII, the folding of which has been described earlier (Törrönen et al., 1994). XYNI is a smaller molecule than XYNII. XYNI is composed of 178 amino acid residues, whereas XYNII contains 190 residues. The van der Waals volume calculated with the program VOIDOO (Kleywegt & Jones, 1994) is 17 320 Å^3 for XYNI and 18 990 Å^3 for XYNII. In a comparison of amino acid sequences and structures it can be noted that XYNI is shorter at the N-terminus and the structure lacks the first β-strand which exists in XYNII (Figure 2). We have described the shape of the overall structure as a "right hand" (Törrönen et al., 1994). The two β-sheets form fingers, and a twisted pair from one β-sheet and the α-helix form a "palm". The long loop between β-strands B7 and B8 makes a "thumb" and a part of the

```
                B1        B2       A2         A3        B3
                      ------>   ---->      ------>   ------>
XYNI              ASINYDQNYQT.GGQVSYSPS.NTGFSVNWNTQDDFVVGVGWTTGSS.A 46
XYNII   QTIQPGTGYNNGYFYSYWNDGHGGVTYTNGPGGQFSVNWSNSGNFVGGKGWQPGTKNK 58
              --->     ----->     ---->     ---->     ------>

             A5          B5          B6b   B6a  cord       B9     B8
          -------->   --------->    -----> -->       -> ---->  ---
XYNI    PINFGGSFSVNSGTGLLSVYGWSTNPLVEYYIMEDNHNY.PA.QGTVKGTVTSDGATY 103
XYNII   VINFSGSYNPN.GNSYLSVYGWSRNPLIEYYIVENFGTYNPSTGATKLGEVTSDGSVY 116
          ---------->   -------->    -----> -->           --->    --
                                     *

                   thumb       B7          A6    helix            B4
          ------>          ------>        --> ==========         --
XYNI    TIWENTRVNEPSIQGTATFNQYISVRNSPRTSGTVTVQNHFNAWASLGLHLGQMNYQV 162
XYNII   DIYRTQRVNQPSIIGTATFYQYWSVRRNHRSSGSVNTANHFNAWAQQGLTLGTMDYQI 175
          ------>          --------->      ---> ==========        ---

                   A4
          -----> --------->
XYNI    VAVEGWGGSGSASQSVSN  178
XYNII   VAVEGYFSSGSASITVS   190
          --->   ------>
            *
```

FIGURE 2: Comparison of the amino acid sequences of XYNI and XYNII together with secondary structure assignment. β-strands are marked as with arrows; an α-helices, as double dashed lines. In addition the positions of the "cord" and the "thumb" are shown. The catalytic residues are marked with asterisks.

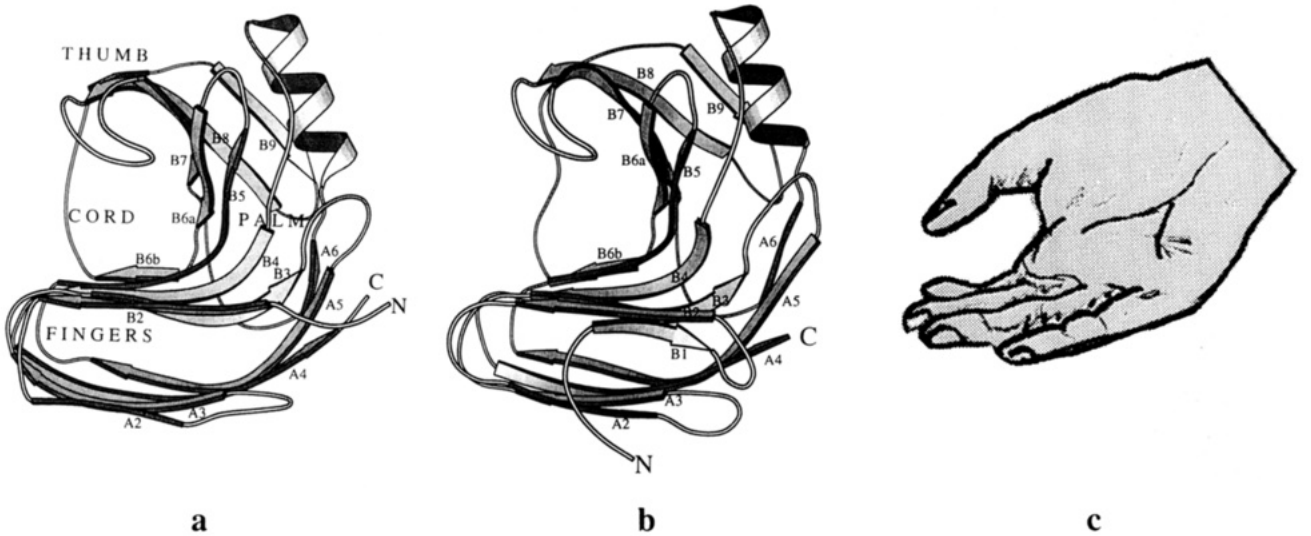

FIGURE 3: Overall structures of XYNI (a) and XYNII (b) (drawn using MOLSCRIPT; Kraulis, 1991). The analogy with the right hand (c) is shown.

loop between β-strands B6a and B9 forms a "cord", which crosses the cleft on one side (Figure 3).

The rise in pH only changes the overall structure of XYNII slightly. The rms difference between the pH 4.5 and pH 6.0 structures is about 0.09 Å, and that between the pH 4.5 and pH 6.5 structures is about 0.14 Å (calculated from the positions of Cα atoms). However, the rms deviation is observed to be about 0.24 Å between two XYNII molecules (A and B in an asymmetric unit) at all three pHs. When comparing XYNI and XYNII structures, we found that XYNII molecule B resembles XYNI more than does molecule A (rms differences of 1.05 and 1.40 Å, respectively). However, when the pH increases to 6.5, the rms difference between XYNII molecule A and XYNI decreases (from 1.40 Å to 1.05 Å), whereas no change in rms deviation between XYNII molecule B and XYNI was observed. The deviations between XYNI and XYNII may be partly explained by the variation in the position of the thumb. In XYNI, the thumb closes the cleft formed on the concave side of the twisted β-sheets. The shortest distance, i.e., that between Cγ of Pro113$_{XYNI}$ (from the thumb) and Oη of Tyr9$_{XYNI}$ (from the "fingers"), is only 4.3 Å in the cleft of XYNI. The cleft is also almost closed in molecule B of XYNII, and the shortest distance, i.e., that between Cγ of Pro126$_{XYNII}$ and Cζ2 of Trp18$_{XYNII}$, is 6.7 Å at all measured pHs. In XYNII molecule A, however, the width of the cleft is larger, the distance being about 7.4 Å.

The length and conformation of the cord in XYNI and XYNII were observed to be different. The cord is composed of seven residues (96−102, Tyr-Asn-Pro-Ser-Thr-Gly-Ala) in XYNII but only five (85−89, Tyr-Pro-Ala-Gln-Gly) in XYNI. Although both cords seem to share a similarity in amino acid sequence, the position of the "similar" residues are different (Figure 4). In the XYNI structure the side chain of Tyr85$_{XYNI}$ points to the interior of the protein and is packed against Leu62$_{XYNI}$ and Met79$_{XYNI}$, whereas in the XYNII structure the corresponding Tyr96$_{XYNII}$ is exposed to the solvent and forms a putative carbohydrate binding site at the end of the cleft. In XYNII Pro98$_{XYNII}$ is in about the same position as Tyr85$_{XYNI}$ and is packed against Tyr73$_{XYNII}$,

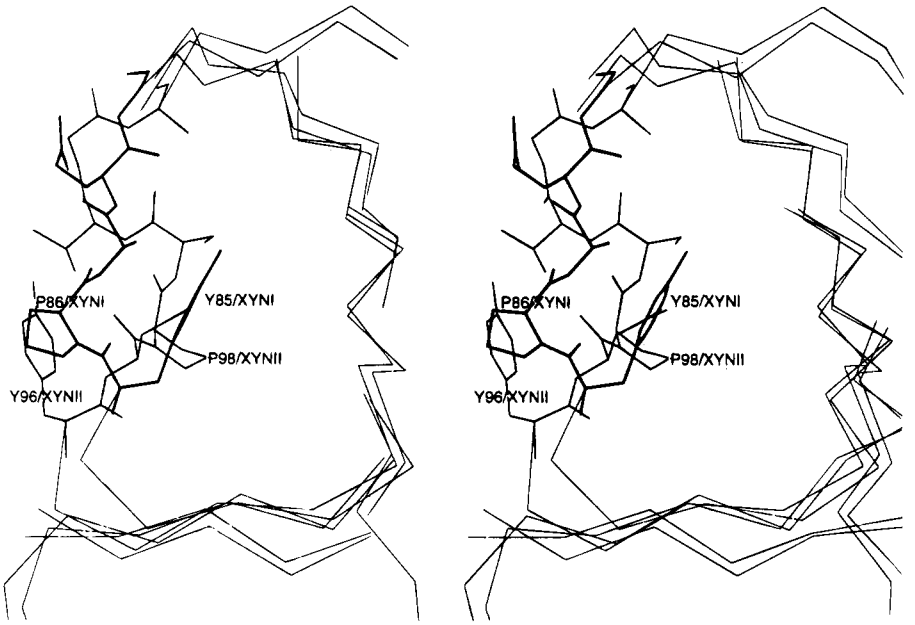

FIGURE 4: Structure of the cords of XYNI (dark bonds) and XYNII (light bonds) superimposed in stereo.

$Val90_{XYNII}$, and $Phe93_{XYNII}$ in the interior of the protein. The XYNII cord has no contacts with neighboring molecules in the crystal whereas the XYNI cord packs against the neighboring molecule. It is difficult to estimate whether this has any effect on the conformation of the cord in XYNI.

Active Sites of XYNI and XYNII. One useful method for evaluating ligand binding is to measure complex structures with substrate or substrate analog/inhibitor attached in the active site. The shorter xylo oligomers or their derivatives seem to have affinities in the millimolar range in family G xylanases (Bray & Clarke, 1992), which may be the reason for the difficulties in obtaining the high-resolution complex structure in the current work. The active sites of family G xylanases probably contain several subsites. We use the notation presented by Bray and Clarke (1992). The cleavage site is between subsites −1 and +1; positive numbers represent reducing end direction, and negative numbers, non-reducing end direction, respectively (Figure 7).

Recently, Wakarchuk et al. (1994) have reported the xylotetraose complex structure of Glu172Cys-xylanase from *Bacillus circulans*. The structure is highly homologous with both XYNI and XYNII (amino acid identity, about 50%). A mutant enzyme was reported to be catalytically inactive, and an electron density for only two xylose residues in the active site was observed (subsites −1 and −2). In this structure Trp9 packs against the xylose ring in subsite −2; Tyr69 and Tyr166 also form hydrogen bonds with the xylose residue. In subsite −1 Arg112 makes hydrogen bonds with the xylose residue. The C1 and O2 of the xylose residue in subsite −1 are close to the putative nucleophile, Glu78.

In the measurement of the X-ray data from XYNII soaked in xylan we can observe weak electron density for one xylose residue in subsite −1 (Figure 5). This measurement can be used only to define the approximate position of one xylose ring in the active site. In order to evaluate the number of subsites in the active site, different xylo oligomer models were built using the program Sybyl and docked to the active sites of both XYNI and XYNII. The directionality of the substrate was obtained from the work of Wakarchuk et al. (1994).

The active site of XYNI probably has space for three subsites, namely, −2, −1, and +1 (Figures 6a and 7). In subsite −2, $Tyr9_{XYNI}$ may pack against the xylose residue, and in subsite +1, $Trp166_{XYNI}$ may pack against the xylose ring. The active site of XYNII is clearly longer than that of XYNI, and it may have five subsites (−2, −1, +1, +2, +3) (Figures 6b and 7). $Trp18_{XYNII}$ may pack against the xylose residue in subsite −2. $Tyr179_{XYNII}$ and $Tyr96_{XYNII}$ may pack against the xylose ring in subsites +2 and +3, respectively.

Catalytic Residues. In a previous paper (Törrönen et al., 1994) we reported that the change of pH causes a clear conformational change in the active site of XYNII; the change in the position of the putative acid/base catalyst $Glu177_{XYNII}$ was particularly striking. In order to analyze this conformational change in more detail, high-resolution data sets were collected at three different pHs: 4.5, 6.0, and 6.5. Minor corrections, concerning some amino acid side chains and water position adjustments, were made in the models by means of refinement. As shown in Figure 8, the conformation of $Glu177_{XYNII}$ is "down" at pH 4.5 and "up" at pH 6.5, whereas we can observe both conformations at pH 6 (relative occupancies, 0.60 and 0.40 for down and up, respectively). The measurement of XYNII with xylan (at pH 5.3) also showed electron density for both conformations. The temperature factors for most amino acid residues in the active site, including catalytic residues, were low (about 15–25 Å^2). Only $Tyr96_{XYNII}$ has a higher *B*-factor, about 33 Å^2. In XYNI the conformation of the corresponding $Glu164_{XYNI}$ is up. Unfortunately, we have not succeeded in obtaining or soaking XYNI crystals at a lower pH in order to investigate whether a conformational change also occurs in this enzyme.

The surroundings of the catalytic residues $Glu75_{XYNI}$ and $Glu86_{XYNII}$ are clearly conserved in the family G xylanases. This cluster contains five conserved residues: $Tyr66_{XYNI}$/$Tyr77_{XYNII}$, $Trp68_{XYNI}$/$Trp79_{XYNII}$, $Tyr77_{XYNI}$/$Tyr88_{XYNII}$, $Gln123_{XYNI}$/$Gln136_{XYNII}$, and $Tyr158_{XYNI}$/ $Tyr171_{XYNII}$. As shown by Wakarchuk et al. (1994), $Tyr66_{XYNI}$/$Tyr77_{XYNII}$ and $Tyr158_{XYNI}$/$Tyr171_{XYNII}$ take part in ligand binding. However, it is also probable that these residues are important in

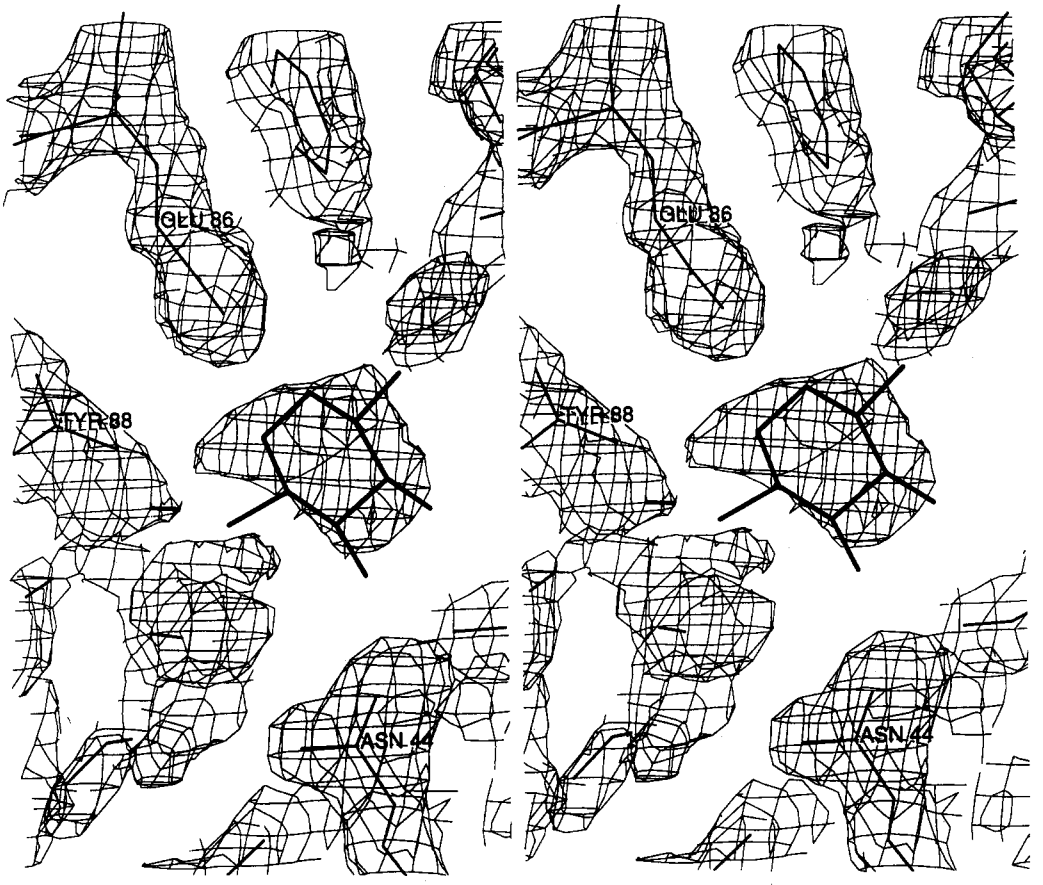

FIGURE 5: $2F_o - F_c$ map at 2.0-Å resolution (contoured at 0.8σ) of XYNII soaked with xylan in stereo. A portion of the map shows the density at the −1 subsites. The model of xylose is shown as a reference. No ligand or water molecules in the active site were used for calculation of the map.

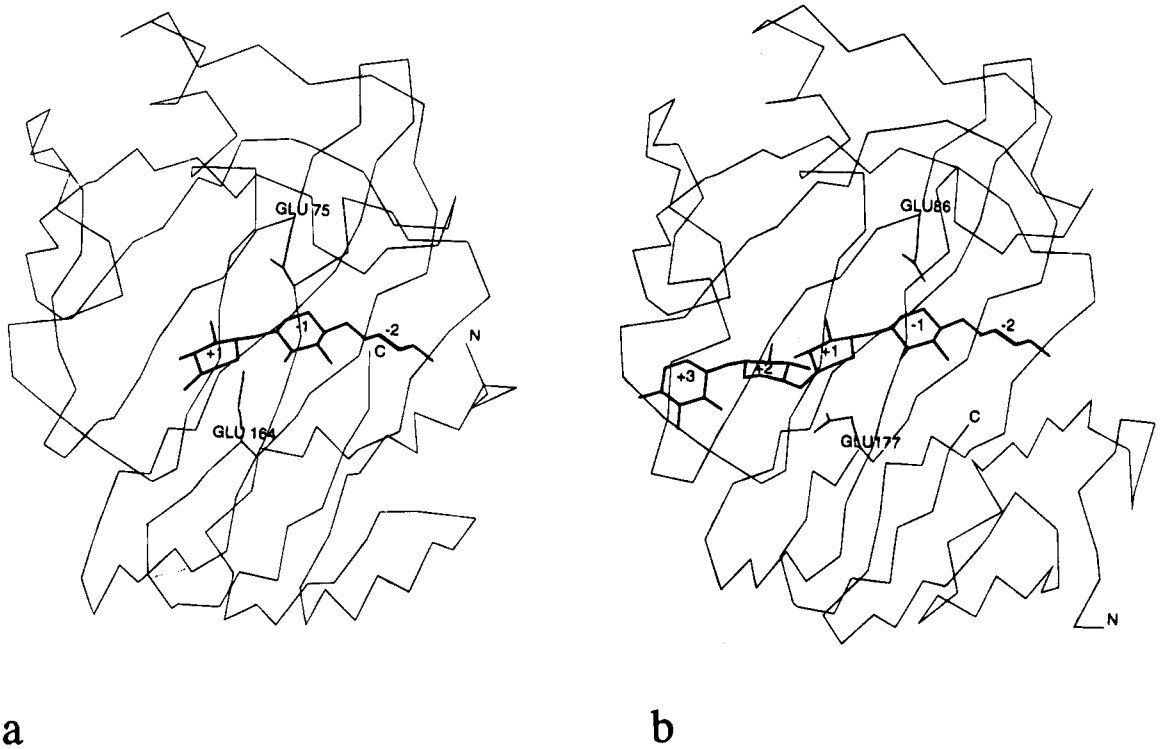

FIGURE 6: Active site of (a) XYNI and (b) XYNII together with the modeled substrate. The putative subsites are numbered.

fine tuning the catalytic properties of $Glu75_{XYNI}$/$Glu86_{XYNII}$. The hydrogen-bonding network is shown in Figure 9. The position of $Gln123_{XYNI}$/$Gln136_{XYNII}$ is the same in all structures. There is a large variation in the strong hydrogen bond between Oη of $Tyr77_{XYNII}$ and Oϵ2 of the catalytic glutamic acid $Glu86_{XYNII}$ in molecules A and B of XYNII.

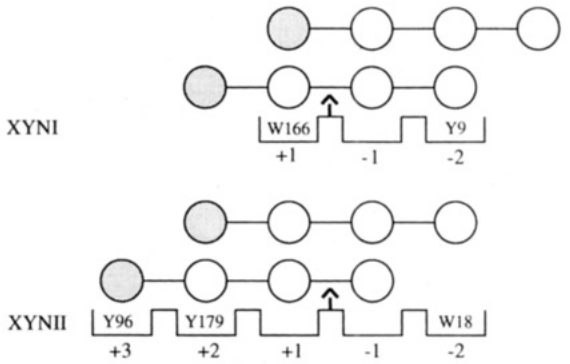

FIGURE 7: Schematic model of the active sites of XYNI and XYNII. Different subsites are numbered. Positive numbers are used for the reducing end, and negative numbers are used for the nonreducing end. Different binding possibilities of xylotetraose are shown. The circles represent xylose units. The circle representing the reducing-end xylose is filled.

In the native structure (pH 4.5) this hydrogen bond length is 2.9 Å in molecule A and 3.3 Å in molecule B, whereas in the pH 6.5 structure the bond length is 2.7 Å in both molecules. We have previously (Törrönen et al., 1994) pointed out the importance of $Tyr88_{XYNII}$ in XYNII structure to work as a link between the two catalytic residues ($Glu86_{XYNII}$ and $Glu177_{XYNII}$). The conformational change in XYNII alters the hydrogen bond of Oη of $Tyr88_{XYNII}$ from Oϵ2 of $Glu86_{XYNII}$ (3.0−3.2 Å) to Oϵ2 of $Glu177_{XYNII}$ (2.8−2.9 Å). In XYNI Oη of $Tyr77_{XYNI}$ makes a hydrogen bond to Oϵ2 of $Glu164_{XYNI}$ (3.3 Å), which corresponds to the similar situation observed in XYNII at a higher pH.

The surroundings of the other catalytic residues $Glu164_{XYNI}$ and $Glu177_{XYNII}$, are much less conserved. An important residue here is $Asp33_{XYNI}$/$Asn44_{XYNII}$. Oδ1 of $Asp33_{XYNI}$ is very close to Oϵ1 of $Glu164_{XYNI}$ (2.9 Å), and it is likely that a proton exists between these two acidic residues. The proton is probably attached to $Asp33_{XYNI}$. In XYNII $Asn44_{XYNII}$ forms a hydrogen bond to $Glu177_{XYNII}$, but the distance is longer than the corresponding distance in XYNI. This hydrogen bond (3.4−3.6 Å) is observed in both conformations of XYNII. In XYNII Oϵ2 of Glu177 does not form any hydrogen bonds at pH 4.5, and thus we believe it to be protonated.

DISCUSSION

It is not clear why the fungus *Trichoderma reesei* produces two structurally similar *endo*-1,4-xylanases, both capable of hydrolyzing the backbone of xylan. However, recent enzymological studies have revealed various differences in the functional properties of these enzymes (Tenkanen et al., 1992; Biely et al., 1993), which may be related to the complexibility of the substrate. This study of the three-dimensional structures of both XYNI and XYNII may give us a better basis for understanding the different functional and catalytic properties of these proteins.

Family G xylanases have been described as acidic and alkaline xylanases according to their isoelectric points. Acidic xylanases (pI < 5.0) have slightly lower pH optima (pH ca. 3−4) than the alkaline (pI > 7) ones (pH ca. 4−5). The number of available sequences of alkaline xylanases is higher than that of the acidic, which seem to be mostly of fungal origin. The isoelectric point of XYNI is 5.2, and that of XYNII is 9.0; i.e., these proteins represent acidic and alkaline xylanases, respectively. The number of histidine and aspartic and glutamic acid residues is almost equal in XYNI and XYNII. The clear difference is in the number of lysine and arginine residues. In XYNI there are only four such residues, whereas in XYNII they number 10. An inspection of the structure of XYNII reveals that these positively charged residues are situated mainly at both sides of the thumb. It is noteworthy that no charged residues exist in the convex finger-forming surface of the β-sheet. This surface is rich in serine and threonine residues (Törrönen et al., 1994). It is difficult to estimate whether the excess of positively charged residues in XYNII has any functional role. However, we could speculate that some of the positively charged residues may interact with acidic 4-*O*-methylglucuronic acid substituents of xylan.

The acidic xylanase XYNI is active in the pH range of 3−6, having maximum activity at about 3.5, whereas the alkaline XYNII is active in a larger pH range from 4 to 8, having a maximum at about 5.3. The pH optimum depends mostly on the properties of the acid/base catalyst $Glu164_{XYNI}$/$Glu177_{XYNII}$. The conformational change observed at pH 6.5 in XYNII is able to place the carboxylate group of $Glu177_{XYNII}$ in a totally different position, thus leading to the change in its pK_a value. We believe that this property is able to increase the active pH range of XYNII. Unfortunately we have not been able to demonstrate whether a similar change also occurs in XYNI. The observed conformation of XYNI resembles that of XYNII at pH 6.5.

The pH optimum difference between XYNI and XYNII may be explained by the variation in the hydrogen bonding of the $Glu164_{XYNI}$/$Glu177_{XYNII}$ residue. In XYNI, $Asp33_{XYNI}$ makes a strong hydrogen bond (2.9 Å) to $Glu164_{XYNI}$. This probably lowers the pK_a value of this glutamic acid. In XYNII, on the other hand, there is an asparagine residue (Asn44) in place of $Asp33_{XYNI}$. The hydrogen bond between $Asn44_{XYNII}$ and $Glu177_{XYNII}$ appears to be much longer (3.4−3.7 Å) than the corresponding one in XYNI, and the interaction between the residues is weaker. This probably raises the pK_a value of $Glu177_{XYNII}$ and also affects the pH optimum of the enzyme. It should be pointed out that all acidic xylanases of family G seem to have an aspartate residue, and alkaline ones have an asparagine residue, in place of $Asp33_{XYNI}$/ $Asn44_{XYNII}$. The *Scizophillum commune* xylanase makes a link between the acidic and the alkaline xylanases. It has previously been grouped as an alkaline xylanase according to the HCA sequence comparison, but the pI of this enzyme was reported to be 4.5 (Oku et al., 1993). The pH optimum of this enzyme, however, follows that of the alkaline xylanases rather than the acidic ones (Paice et al., 1978). From the sequence alignment it can be observed that the corresponding residue is asparagine in *S. commune* (Wakarchuk et al., 1994).

The subsite architecture in the active site cleft in XYNI and XYNII seems to be clearly different. The active site of XYNI is tighter than that of XYNII. The tightness is affected mostly by the movement of the thumb, which closes the active site at the position of subsites −2 and −1. In the XYNII structure we can observe that the thumb is cabable of moving by at least 0.7 Å. In XYNI the thumb closes the cleft even more than in XYNII. This was also observed by Campbell et al. (1993), who found that the largest differences between xylanases from *Bacillus circulans* and *Trichoderma harzianum* are in just the position of the "lip".

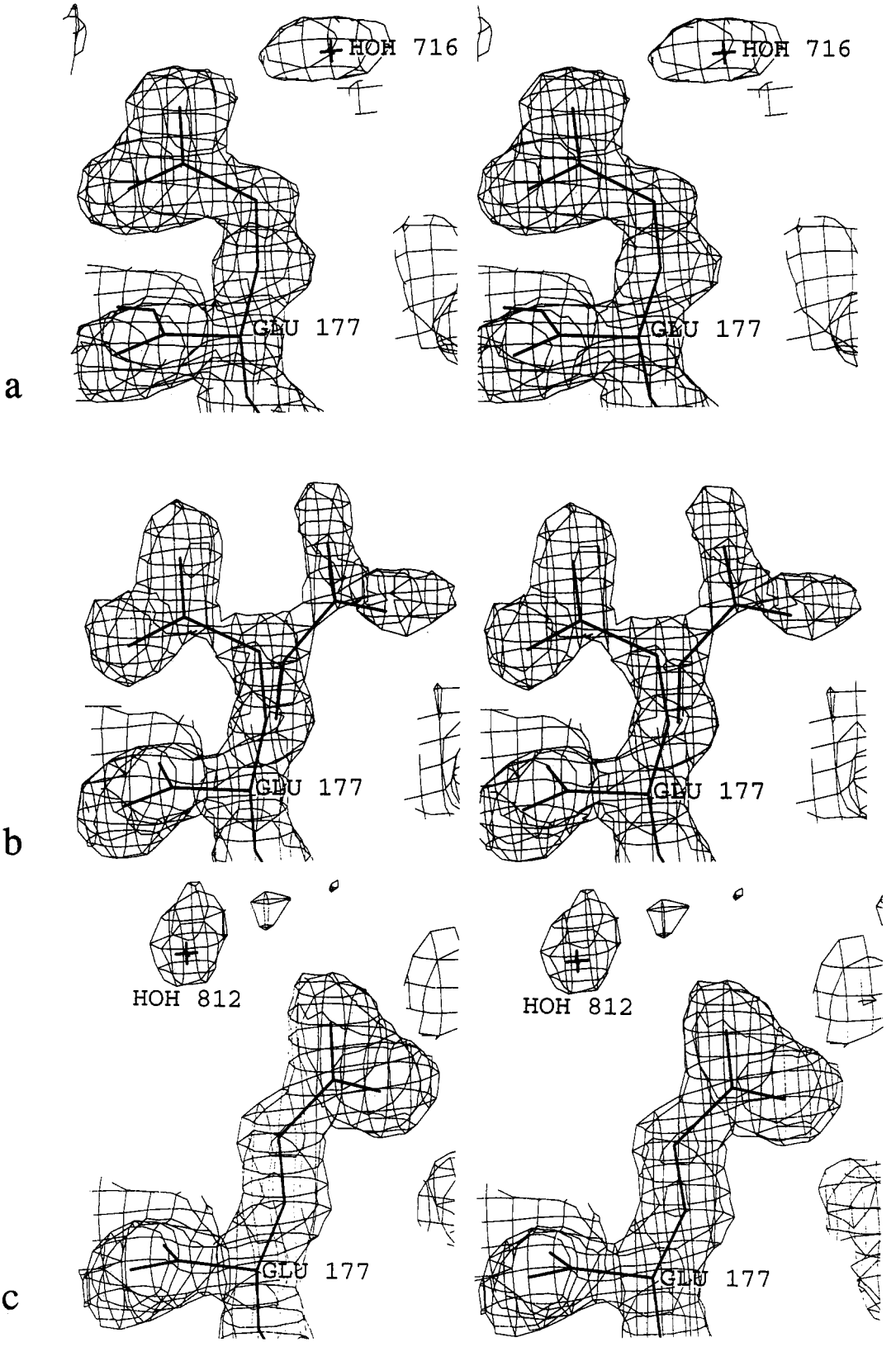

FIGURE 8: Final $2F_o - F_c$ electron density maps at 1.5-Å resolution (1σ level) for Glu177 of XYNII at pH 4.5 (a), pH 6.0 (b), and pH 6.5 (c).

The number of subsites in XYNI was concluded to be three, whereas five subsites could be suggested for XYNII. In XYNI the reducing-end site is composed of only one subsite (+1), but the nonreducing end has two subsites. This suggests that the ligand binding is directed to the nonreducing end in the XYNI structure. Biely et al. (1993) have reported that XYNI cleaves xylotetraose at the first and second glycosidic linkages from the reducing end. This can be easily explained by the three-subsite model for XYNI, where four xylose units containing xylotetraose would have two possibilities of fully occupying the active site: one xylose unit would lay outside the subsites at either the reducing or the

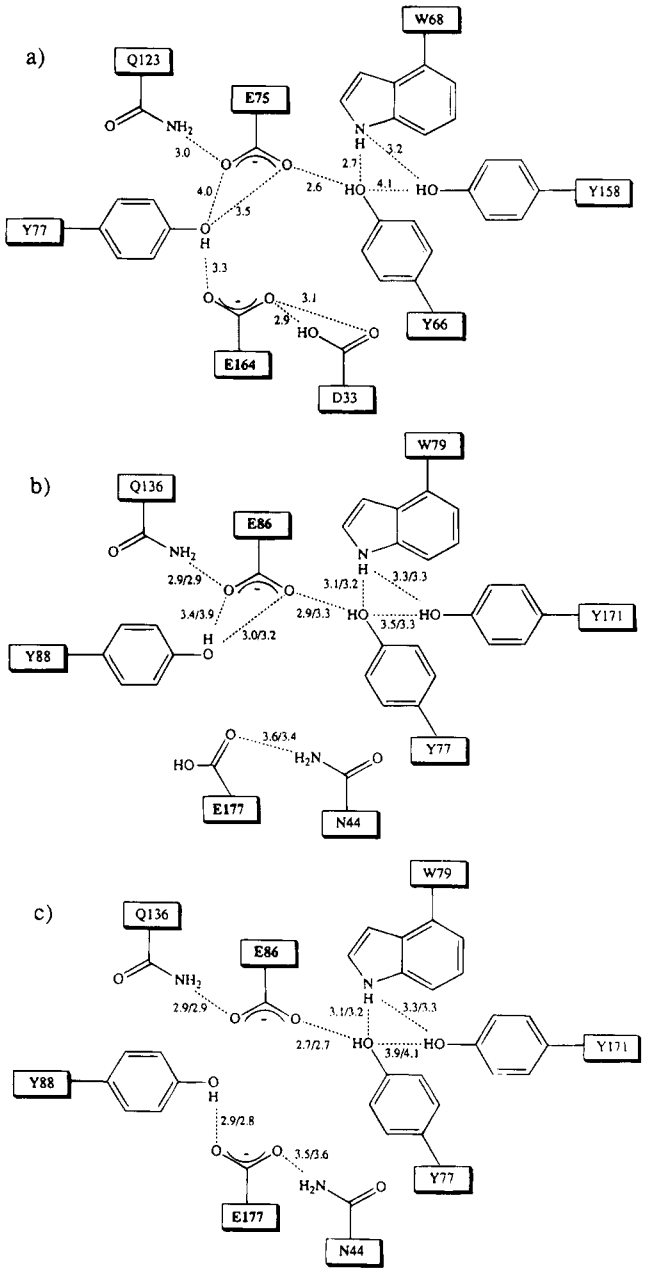

FIGURE 9: Hydrogen bonding around the catalytic residues: (a) XYNI and (b) XYNII at pH 4.5 and (c) XYNII at pH 6.5. The distances between non-hydrogen atoms are given. For XYNII the first number corresponds to the distance observed in molecule A, and the second number, that observed in molecule B.

nonreducing site (Figure 7). On the other hand, XYNI clearly prefers to cleave xylopentaose at the second glycosidic linkage (Biely et al., 1993). Thus the five units containing xylopentaose would occupy the subsites of XYNI in a manner in which the xylose residues at both ends would fall away from the active site.

There are five putative subsites in XYNII, three (+1, +2, +3) at the reducing end and two at the nonreducing end (−1, −2). The larger number of subsites at the reducing end would probably direct ligand binding toward the reducing end of the xylan chain. Biely et al. (1993) have found that xylotetraose is cleaved at the second and third glycosidic linkages from the reducing end. This could be explained by assuming that the xylotetraose is bound to XYNII in a manner in which the first or the last subsite is empty. The remaining four subsites would participate in ligand binding (Figure 7). Xylopentaose, on the other hand, is cleaved at the second, third, or fourth glycosidic linkages (Biely et al., 1993), which would mean either that all the subsites are occupied or that site −2 or +3 is empty and the rest are occupied.

Tenkanen et al. (1992) have shown that XYNI is capable of hydrolyzing acetylated glucuronoxylan into smaller units than XYNII, whereas XYNII hydrolyzes deacetylated glucuronoxylan better. It is likely that XYNI, as a smaller enzyme with a smaller active site, is able to reach more buried internal glycosidic bonds better than XYNII. Thus XYNI is capable of hydrolyzing xylan further than XYNII.

Both XYNI and XYNII belong to the G/11 glycosidase family, which consists of highly homologous *endo*-1,4-xylanases. Family G xylanases have been shown to be retaining enzymes; i.e., they retain the configuration of the anomeric carbon C1 (Gebler et al., 1992). Many retaining enzymes also catalyze glycosyl transfer between two substrate molecules (Sinnott, 1990). It has been reported that both XYNI and XYNII have β-1,4-glycosyltransferase activity, but the XYNII activity is much more evident (Tenkanen et al., 1992). XYNI is also repored to have β-1,3-glycosyltransferase activity (Biely et al., 1993). The differences between XYNI and XYNII in glycosyltransferase activity could be explained by comparing the distribution of subsites in the enzymes. In *trans*-glycosylation the reaction intermediate, carbonium ion, would occupy the subsite −1, and the rest of the intermediate molecule would bind to subsite −2 or even further. The second xylo oligomer, taking part in the *trans*-glycosylation reaction, would occupy subsites +1, +2, etc. In XYNI there is only one subsite, +1, and the xylo oligomer binding is probably very weak, whereas in XYNII there are three subsites (+1, +2, +3), which makes the binding of the second oligomer more probable and *trans*-glycosylation more likely to occur.

ACKNOWLEDGMENT

We thank Ms. Reetta Kallio for her skillful technical assistance.

REFERENCES

Biely, P., Vrsanska, M., Kremnicky, L., Tenkanen, M., Poutanen, K., & Hayn, M. (1993) in *Proceedings of the Second TRICEL Symposium on Trichoderma Cellulases and Other Hydrolases* (Suominen, P., & Reinikainen, T., Eds.) pp 125−135, Foundation for Biotechnical and Industrial Fermentation Research, Helsinki.

Bray, M. R., & Clarke, A. J. (1992) *Eur. J. Biochem. 204,* 191−196.

Brünger, A. T., Kuriyan, J., & Karplus, M. (1987) *Science 235,* 458−460.

Campbell, R. L., Rose, D. R., Wakarchuk, W. W., To, R., Sung, W., & Yaguchi, M. (1993) in *Proceedings of the Second TRICEL Symposium on Trichoderma Cellulases and Other Hydrolases* (Suominen, P., & Reinikainen, T., Eds.) pp 63−72, Foundation for Biotechnical and Industrial Fermentation Research, Helsinki.

Davies, G. J., Dodson, G. G., Hubbard, R. E., Tolley, S. P., Dauter, Z., Wilson, K. S., Hjort, C., Mikkelsen, J. M., Rasmussen, G., & Schülein, M. (1993) *Nature 365,* 362−364.

Divne, C., Ståhlberg, J., Reinikainen, T., Ruohonen, L., Pettersson, G., Knowles, J. K. C., Teeri, T. T., & Jones, T. A. (1994) *Science 265,* 524−528.

Engh, R. A., & Huber, R. (1991) *Acta Crystallogr. A47,* 392–400.

Evans, S. V. (1993) *J. Mol. Graphics 11,* 134–138.

Gebler, J., Glikes, N. R., Claeyssen, M., Wilson, D. B., Béguin, P., Wakarchuk, W. W., Kilburn, D. G., Miller, R. C., Jr., Warren, R. A. J., & Withers, S. G. (1992) *J. Biol. Chem. 267,* 12559–12561.

Gilkes, N. R., Henrissat, B., Kilburn, D. G., Miller, R. C., & Warren, R. A. J. (1991) *Microbiol. Rev. 55,* 303–315.

Henrissat, B. (1991) *Biochem. J. 280,* 309–316.

Henrissat, B., & Bairoch, A. (1993) *Biochem. J. 293,* 781–788.

Jones, T. A., Zou, J.-Y., Cowan, S. W., & Kjeldgaard, M. (1991) *Acta Crystallogr. A47,* 110–119.

Juy, M., Amit, A. G., Alzari, P. M., Poljak, R. J., Claeyssens, M., Beguin, P., & Aubert, J.-P. (1992) *Nature 357,* 89–91.

Keitel, T., Simon, O., Borriss, R., & Heinemann, U. (1993) *Proc. Natl. Acad. Sci. U.S.A. 90,* 5287–5291.

Kleywegt, G. J., & Jones, T. A. (1994) *Acta Crystallogr. D50,* 178–185.

Ko, E. P., Akatsuka, H., Moriyama, H., Shinmyo, A., Hata, Y., Katsube, Y., Urabe, I., & Okada, H. (1992) *Biochem. J. 288,* 117–121.

Kraulis, P. J. (1991) *J. Appl. Crystallogr. 24,* 946–950.

Okada, H. (1989) *Adv. Protein Des. 12,* 81–86.

Oku, T., Roy, C., Watson, D. C., Wakarchuk, W., Campbell, R., Yaguchi, M., Jurasek, L., & Paice, M. G. (1993) *FEBS Lett. 334,* 296–300.

Paice, M. G., Jurasek, L., Carpenter, M. R., & Smillie, L. B. (1978) *Appl. Environ. Microbiol. 36,* 802–808.

Ramakrishnan, C., & Ramachandran, G. N. (1965) *Biophys. J. 5,* 909–933.

Rouvinen, J., Bergfors, T., Teeri, T., Knowles, J. K. C., & Jones, T. A. (1990) *Science 249,* 380–386.

Sinnott, M. L. (1990) *Chem. Rev. 90,* 1171–1202.

Spezio, M. L., Wilson, D. B., & Karplus, P. A. (1993) *Biochemistry 32,* 9906–9916.

Sundberg, M., & Poutanen, K. (1991) *Biotechnol. Appl. Biochem. 13,* 1–11.

Tenkanen, M., Puls, J., & Poutanen, K. (1992) *Enzyme Microb. Technol. 14,* 566–574.

Törrönen, A., Mach, R. L., Messner, R., Gonzalez, R., Kalkkinen, N., Harkki, A., & Kubicek, C. P. (1992) *Bio/Technology 10,* 1461–1465.

Törrönen, A., Kubicek, C. P., & Henrissat, B. (1993a) *FEBS Lett. 321,* 135–139.

Törrönen, A., Rouvinen, J., Ahlgren, M., Harkki, A., & Visuri, K. (1993b) *J. Mol. Biol. 233,* 313–316.

Törrönen, A., Harkki, A., & Rouvinen, J. (1994) *EMBO J. 13,* 2493–1501.

Varghese, J. N., Garrett, T. P. J., Colman, P. M., Chen, L., Høj, P. B., & Fincher, G. B. (1994) *Proc. Natl. Acad. Sci. U.S.A. 91,* 2785–2789.

Voointholt, R., Kosters, M. T., Vegter, G., Vriend, G., & Hol, W. G. J. (1989) *J. Mol. Graphics 7,* 243–245.

Wakarchuk, W. W., Campbell, R. L., Sung, W. L., Davodi, J., & Yaguchi, M. (1994) *Protein Sci. 3,* 467–475.

BI9419644